The hydrology of the proglacial zone of a high-Arctic glacier (Finsterwalderbreen, Svalbard): Sub-surface water fluxes and complete water budget.

Richard Cooper[a]

Richard Hodgkins[b1]

Jemma Wadham[c]

Martyn Tranter[c]

[a] The Macaulay Institute, Craigiebuckler, Aberdeen, AB15 8QH, U.K.

[b] Polar and Alpine Research Centre, Department of Geography, Loughborough University, Leicestershire, LE11 3TU, U.K.

[c] Bristol Glaciology Centre, School of Geographical Sciences, University of Bristol, Bristol, BS8 1SS, U.K.

[1]Corresponding author: r.hodgkins@lboro.ac.uk, tel. +44-(0)1509-222753, fax +44-(0)1509-223930.

Abstract

Proglacial areas receive fluxes of glacial meltwater in addition to their own hydrological inputs and outputs, while in high latitudes the seasonal development of the active layer also affects their hydrology. This paper supplements a previous study of the surface and atmospheric water fluxes in the proglacial area of the Svalbard glacier Finsterwalderbreen (77° N), by focusing on the sub-surface water fluxes of the active layer, and bringing together all the components of the proglacial water balance over a complete annual cycle. Particular attention is given to the transitional zone between the moraine complex and the flat sandur. Sub-surface water in the moraine complex (sourced mainly from snowmelt, lake drainage and active-layer thawing), is exchanged with sub-surface water from the sandur (sourced mainly from glacier-derived snow- and icemelt), across a largely distinct boundary. Hydraulic head and specific discharge were monitored in a transect of wells spanning this boundary. A hydraulic gradient from the moraine complex to the sandur is maintained throughout the melt season, although this is reversed first briefly when glacial runoff floods the sandur, and then diurnally from mid-melt-season, as peak daily flow in the proglacial channel network drives sub-surface water in the sandur towards the moraine complex. It is estimated that the active layer does not freeze up until mid-December at this location, so that sub-surface water flow may be maintained for months after the cessation of surface runoff. However, the magnitude of sub-surface flow is very small: the total, annual flux from the moraine complex to the sandur is 11 mm, compared with 1073 mm of total, annual runoff from the whole catchment (glacier included). Furthermore, when considering the water balance of the entire proglacial area, there are unlikely to be significant, seasonal storage changes in the active layer.

Key words proglacial, active layer, hydraulic conductivity, water balance, water budget, Svalbard.

PACS codes 92.40.Vq, 92.40.We, 92.40.Zg

1. Introduction

Proglacial areas are expanding globally as a consequence of sustained glacier retreat (Zemp et al., 2008), and can be characterized as highly dynamic fluvial environments (Warburton, 1999). Given the intractability of most proglacial areas, and the complex experimental design necessary for monitoring multiple hydrological fluxes over sustained periods in such dynamic environments, it is unsurprising that still very few comprehensive water balance studies are available for glacierized catchments as a whole, or for proglacial areas in particular. Water balances for glaciers themselves can be derived from mass-balance data assuming that inter-annual storage is insignificant (e.g. Hagen et al., 2003), but these shed little light on the hydrological functioning of catchments, and on the interaction and relative contributions of different drainage pathways and potential stores. As water and sediment fluxes from glaciers globally are likely to increase over the coming decades (ACIA, 2004; Meehl et al., 2007) an enhanced understanding of the hydrological functioning of proglacial areas would be beneficial: the purpose of this paper is to contribute to this understanding – building on a previous paper which dealt with surface and atmospheric water fluxes in a proglacial area in the Norwegian high-Arctic archipelago of Svalbard (Hodgkins et al., 2009) – by analyzing sub-surface (active-layer) water fluxes and bringing together the complete water balance over an annual cycle.

Studies of sub-surface hydrology in Svalbard have tended to focus on sub-permafrost groundwater (e.g. Haldorsen et al., 1996; Booji et al., 1998; Haldorsen and Heim, 1999), with relatively little attention paid to water flow within the active layer. However, results from several hydrochemical studies suggest that the annual formation of the active layer is hydrologically significant: observations indicate that the annual formation of the active layer in Svalbard typically commences following snowpack recession in early June (Herz & Andreas, 1966; Stäblein, 1971), when mean air temperatures begin to rise consistently above zero (Hanssen-Bauer et al., 1990). Downward-thawing velocities are initially high, although

71 variations in microtopography and the persistence of patchy snow cover may result in the
72 development of an irregular permafrost table with thawed troughs and frozen ridges, though
73 this irregularity tends to even out as the melt season progresses. The potential for sub-surface
74 water storage and flow in the active layer increases in line with the gradual increase in the
75 depth of the permafrost table, which constitutes the lower boundary layer for water
76 movement (Pecher, 1994). Sub-surface flow in the active layer may increasingly contribute to
77 throughputs of runoff in the proglacial zone as the melt season progresses (Pecher, 1994;
78 Hodson et al., 1998); this effect may be enhanced following precipitation events, due to the
79 displacement of sub-surface water by infiltrating precipitation.
80 Available studies indicate that Arctic catchments often exhibit a pattern in which
81 runoff appears significantly to exceed precipitation (Killingtveit et al., 2003). This can be
82 attributed to a combination of measurement errors, non-representative locations of
83 precipitation stations, and net glacial ablation. Førland et al. (1997) considered that
84 precipitation underestimation for upland areas by coastally-located gauges may fully account
85 for the discrepancy between precipitation measured at Ny-Ålesund and runoff from the
86 nearby Bayelva catchment. Groundwater storage has often been regarded as insignificant in
87 glacierized catchments in Svalbard (e.g. Hagen et al., 2003), usually owing to the presence of
88 permafrost, although there is little evidence available and groundwater springs are not
89 unusual (Haldorsen and Heim, 1999). With regards to the active layer itself, the observation
90 that total evaporation at elevations <50 m above sea level (a.s.l.) in Svalbard may exceed
91 precipitation by up to about 160% during the summer indicates that water storage there is
92 often sufficient to maintain the rate of evaporation during dry periods (Harding and Lloyd,
93 1997).
94

1.1. Aims

The purpose of this paper is to quantify and analyze the sub-surface hydrology of the proglacial area of a high-Arctic glacier, focusing in general on water fluxes in the active layer, and in particular on the transitional zone between the moraine complex and the sandur (see Section 2, 'Study site description'). Time series of both active layer development and of hydraulic head in the active layer were acquired by in-situ monitoring over the course of the 1999 melt season, in order to elucidate sub-surface hydraulic gradients and flow paths in the transitional zone. The saturated hydraulic conductivity of the sediments comprising the active layer was assessed, in order to enable the time series of hydraulic head to be used to determine specific discharge at the boundary between the moraine complex and the sandur, and thus facilitate the calculation of total sub-surface water fluxes to and from the moraine complex. These fluxes will then be combined with previously-determined surface and atmospheric fluxes (Hodgkins et al., 2009) to present a comprehensive, annual, proglacial water balance.

2. Study site description

The proglacial zone of Finsterwalderbreen is located at 77º 31´ N, 15º 19´ E in the Norwegian High Arctic archipelago of Svalbard (Fig. 1). It is part of a catchment situated on the southern side of Van Keulenfjorden which drains northwards to the sea from a maximum elevation of 1065 m a.s.l. The catchment is constrained to the east, south and west by high mountain ridges, and has a total area of 65.7 km^2, of which 43.5 km^2 is currently glacierized. The non-glacierized part of the catchment comprises steep, scree-covered mountain slopes, with the exception of the proglacial zone itself, which consists of a flat sandur (mostly between 10–20 m a.s.l.) surrounded by a moraine complex (mostly between 20–50 m a.s.l.), situated between the glacier terminus and the coastline of Van Keulenfjorden (Fig. 1). The characteristics of the proglacial zone have been described in detail in Hodgkins et al. (2009).

Of particular interest for this paper is the transitional zone between the moraine complex and the sandur: the former consists of a series of compounded ridges (marking the limits of previous advances) enclosing a hummocky terrain of kames and kettles (many of which contain small lakes) composed largely of glacial diamicton, interspersed with relict outwash terraces; the latter is a relatively uniform, low-gradient surface, composed largely of fluvial sediments, across which glacier meltwater streams braid extensively (Fig. 1). Sub-surface waters from the moraine complex, sourced mainly from snowmelt, lake drainage and active-layer thawing, are exchanged with those from the sandur, sourced mainly from glacier-derived snow- and icemelt, across the largely distinct boundary between the two; this exchange was the focus of field measurements, described in Section 3.

3. Methods: Determination of sub-surface water fluxes between the moraine complex and the sandur

3.1. Hydraulic head monitoring

Hydraulic head was monitored for a total of 36 days, from 19:00 on day 192 (11 July) to 11:00 on day 227 (15 August). At the start of the monitoring period, five PVC-tube monitoring wells (Fig. 2) were sited along a gently-sloping transect spanning the transitional zone, approximately 1 km downstream from the glacier terminus (Fig. 1). The characteristics of these wells have been described in detail by Cooper et al. (2002), in a study of the hydrochemistry of waters in the active layer. Following a period of equilibration, Druck PDCR1830 pressure transducers were used to sample pressure head in each well at 20-s intervals, and record hourly means (potential error ±0.1%). Pressure-head values were calibrated with a measurement of elevation head derived from field surveying, to give the record of hydraulic head. No significant net change in the elevation of the sandur due to aggradation or degradation was detected at the wells transect (with one exception, noted in Section 4.1). The potential error range for hydraulic head is estimated to be ±5%. Active

147 layer depth during the monitoring period was measured every 2–6 days by driving a steel
148 stake into the ground at each well, until the resistance of the uppermost surface of the
149 permafrost was encountered (estimated error range ±5%).
150
151 ### 3.2. Saturated hydraulic conductivity testing
152 The saturated hydraulic conductivity (K_{sat}) of the sediments comprising the active
153 layer in the transitional zone is required to determine specific discharge, and hence quantify
154 sub-surface water fluxes. K_{sat} (m s^{-1}) was assessed using falling-head slug tests in the
155 monitoring wells (Bouwer and Rice, 1976; Bouwer, 1989) and determined from
156
$$K_{sat} = \frac{R_i^{\,2} \ln(L_r / R_e)}{2L_i} \frac{1}{t} \ln\left(\frac{\psi_0}{\psi_t}\right) \quad (1)$$

157
158 where R_i and R_e are the internal and external radii of the well tubing respectively (m), L_r is
159 the effective radius over which the increase in pressure head is dissipated (m), L_i is the length
160 of the screened intake through which water can enter (m), t is the time since $\psi = \psi_0$ (s), ψ is
161 pressure head in the well (m), ψ_0 is the maximum displacement in pressure head at time $t = 0$
162 (m) and ψ_t is the displacement in pressure head at $t = t$ (m) (Bouwer and Rice, 1976). As L_r is
163 unknown, the dimensionless ratio $\ln(L_r/R_e)$ was estimated from
164
$$\ln\frac{L_r}{R_e} = \left\{ \frac{1.1}{\ln(L_w / R_e)} + \frac{a + b\ln\left[(L_b - L_w)/R_e\right]}{L_i / R_e} \right\}^{-1} \quad (2)$$

165
166
167 where L_w is the distance from the bottom of the well to the water table (m), a and b are
168 dimensionless functions of L_i/R_e and L_b is the distance from the water table to the upper
169 surface of the permafrost (m)(Bouwer, 1989). K_{sat} values obtained in this way ranged from
170 6.01×10^{-5} m s^{-1} for sandur sediments to 4.08×10^{-4} m s^{-1} for moraine complex sediments.
171
172

3.3. Specific discharge and sub-surface water flux calculation

Sub-surface water fluxes, Q ($m^3\ s^{-1}$) (Fig. 3A), were determined as the product of mean hourly values of specific discharge ($m\ s^{-1}$) at the well situated closest to the boundary between the moraine complex and the sandur (Well 4) and the cross-sectional area of that boundary, A (m^2), using

$$Q = \left(K_{sat} \frac{dH}{dL} \right) A \tag{3}$$

where dH/dL is the hydraulic gradient between Wells 4 and 5, determined by dividing the difference in mean hourly values of hydraulic head by the distance between the wells, and A is determined by multiplying the saturated layer depth L_b (m) by the moraine complex-sandur boundary length (7000 m): given the flat nature of the sandur, it is probably reasonable to assume that all of the boundary is active concurrently. Hourly values of L_b were determined from

$$L_b = \psi + \left(L_a - L_s \right) \tag{4}$$

where L_a is the depth of the active layer (m) (the distance from the ground surface to the upper surface of the permafrost) and L_s is the distance from the bottom of the well to the ground surface (m).

3.4. Unmonitored sub-surface water fluxes

As with the surface and atmospheric water fluxes at Finsterwalderbreen discussed in Hodgkins et al. (2009), monitoring of hydraulic head and active layer development commenced some time after the onset of the thaw associated with the 1999 melt season, and ceased some time before the annual freeze-up. Sub-surface water fluxes during these missed intervals may have been significant, particularly during the latter period, since the relationship between decreasing air temperature and refreezing is subject to the zero-curtain

199 effect, whereby the release of latent heat stabilizes the temperature of the active layer at 0 °C
200 for a prolonged period, delaying the progression of the freezing front (Boike et al., 1998).
201 However, the development of a robust annual hydrological budget requires these missed
202 fluxes to be quantified.

203 The first step was to estimate variation in the thickness of the active layer during the
204 pre-monitoring interval. Monitoring-interval data exhibited an almost perfect linear
205 relationship between cumulative, positive, hourly air temperature and active layer depth at all
206 five of the monitoring wells (R^2 values >0.99 in all cases), reflecting the dominance of
207 conductive heat transfer during the melt season. Active layer development at Well 4 was
208 therefore predicted using a linear regression model, constructed from all available input terms
209 for the interval during which active layer depths were monitored, i.e. days 192–227 (11 July–
210 15 August). The second step was to model the freeze-back of the active layer following the
211 cessation of monitoring. Freeze-back at Well 4 was again predicted using regression models,
212 based on significant linear relationships between cumulative, negative, hourly air temperature
213 and the progression of the downward- and upward-moving freezing fronts in the active layer
214 at a comparable site in Svalbard during this interval (Roth and Boike, 2001). Daily,
215 unmonitored, sub-surface water fluxes were then estimated by multiplying values of
216 estimated L_b (a linear function of active layer depth, again using input terms from the
217 monitoring interval – see Equation 4) by the mean value of specific discharge determined
218 during the period of monitoring. A summary of the regression models is provided in Table 1.
219

220 ## 4. Results: Sub-surface water fluxes between the moraine complex and the sandur

221 ### 4.1. Temporal variation in hydraulic head and specific discharge

222 The temporal pattern of hydraulic head during the period of monitoring (Fig. 3A) was
223 characterised by three periods of markedly different behaviour:

(1) From day 192–196 (11–15 July), hydraulic-head values in those wells sited in the moraine complex (Wells 4 and 5) were high and relatively invariable, while values on the sandur (Well 3) were lower and more variable (Fig. 3A; note that Wells 1 and 2 are excluded from the figures and discussion, as their behaviour was almost identical to that of Well 3, so they add no additional insight); a hydraulic gradient was maintained from the moraine complex to the sandur throughout this period.

(2) From day 197–209 (16–28 July), water levels in all of the wells were somewhat higher and more variable than previously. Peak seasonal values of hydraulic head in all of the wells were recorded in the interval from day 199–202 (18 July–21 July), when the surface of the sandur became flooded in response to peak seasonal flow in the proglacial channel network (Wadham et al., 2001; Hodgkins et al., 2009). During this interval, hydraulic-head values in Wells 3 and 4 periodically exceeded those in Well 5, reversing the hydraulic gradient from the moraine complex to the sandur. As the floodwaters subsided, it became apparent that the surface of the sandur had been eroded between Wells 3 and 4, forming a depression into which channel waters were able to flow.

(3) From day 210–227 (29 July–15 August), water levels in Well 3 were elevated in comparison to interval 1, reflecting the routing of a greater proportion of flow down the western margin of the sandur following the peak seasonal, proglacial flow. A greater degree of diurnal variability was recorded in Wells 3 and 4 during interval 3, along with significant temporal variation in peak daily values of hydraulic head. While peak daily hydraulic-head values in Well 4 closely tracked the diurnal pattern of flow in the proglacial channel network with a 1–2 hour delay, those in Well 3 typically exhibited a 10–14 hour delay. Since similar values of hydraulic head were maintained in Wells 3 and 4 throughout this period, the temporal variation in peak daily values resulted in the reversal of the hydraulic gradient on the sandur on a daily basis. However, consistently high values of hydraulic head in Well 5

maintained an overall hydraulic gradient from the moraine complex to the sandur throughout this interval.

Time series of specific discharge at Well 4 are presented in Fig. 3B. The pattern of specific discharge during the period of monitoring was characterised by a trend of fairly constant discharge (ranging from 2.10×10^{-7} m s^{-1} to 1.64×10^{-6} m s^{-1}), punctuated by a short period of recharge (peak value -1.14×10^{-6} m s^{-1}), which occurred in response to peak seasonal flow in the proglacial channel network and reflects the temporary reversal of the hydraulic gradient. The greater degree of diurnal variability in discharge following the period of recharge reflects the daily inflow and outflow of channel waters to and from the depression formed between Wells 3 and 4. High values of peak daily discharge of ~1.40×10^{-6} m s^{-1} on days 221 (9 August) and 226 (14 August) reflect elevated water levels in the moraine complex following heavy rainfall (Hodgkins et al., 2009: Fig. 2).

4.2. Daily and cumulative sub-surface water fluxes

Active layer depth at each well increased linearly throughout the period of monitoring, at a rate of ~0.01 m d^{-1} (Fig. 4A). Significant spatial variation in active layer depth was observed on the sandur, reflecting local variations in channel proximity and thermal erosion. Despite the deepening of the active layer, water levels in the wells sited in the moraine complex remained relatively constant, resulting in a progressive increase in the thickness of the saturated layer as the season progressed.

Total daily sub-surface water fluxes are presented in Fig. 4B. A total cumulative sub-surface water flux of 9.24×10^{3} m^{3} was discharged from the moraine complex to the sandur during the 34-day period from days 193–226 (12 July–14 August). Total daily sub-surface water fluxes were positive throughout this time interval, except for on day 199 (18 July), when 2.04×10^{2} m^{3} was recharged to the moraine complex from the sandur. Very low positive total daily sub-surface water fluxes during the following 2 days reflect shorter, subsequent

periods of recharge. The highest total daily sub-surface water flux was recorded on day 226 (14 August), when 4.69×10^2 m^3 (about 5% of the total cumulative sub-surface water flux) was discharged from the moraine complex to the sandur following heavy rainfall.

Total sub-surface water fluxes outside the monitoring period were estimated as the product of the number of missed days of monitoring and the mean daily sub-surface water flux measured during the period of monitoring (2.72×10^2 m^3). The number of missed days was estimated by subtracting the number of days in the period of monitoring (34) from the number of days during which mean daily air temperatures were consecutively positive: 107 days from 5 June–19 September (Hodgkins et al., 2009: Fig. 2). A cumulative total sub-surface water flux of 1.99×10^4 m^3 is therefore estimated to have been discharged from the moraine complex to the sandur outside the period of monitoring. Adding this missed total to the monitored total gives a total annual sub-surface water flux of 2.91×10^4 m^3, of which about 32 % was monitored.

4.3. Sub-surface water flux uncertainties

Various sources of potential error have been identified concerning the calculation of sub-surface water fluxes, including those associated with the use of instrumentation, field techniques and extrapolation in both space and time. Of these potential sources of error, some are quantifiable and thus susceptible to probabilistic analysis, while others are systematic and more difficult to constrain. For example, the disturbance associated with digging and then back-filling holes for the installation of the monitoring wells into the coarse-grained sediments of the moraine complex probably affected the saturated hydraulic conductivity of the surrounding sediments, but to what extent is unknown. Furthermore, with regard to upscaling from specific-discharge estimates at set points on the boundary between the moraine complex and the sandur to sub-surface water flux estimates for the boundary as a whole, it is acknowledged that values of saturated hydraulic conductivity probably vary

301 significantly across the moraine complex, and that the depth of the active layer and thickness
302 of the saturated layer also probably exhibit significant spatial variability.
303 In view of the above, the sub-surface water fluxes must be viewed as first-order
304 estimates and treated with an appropriate degree of caution, given that it is not possible to
305 determine realistic error estimates with the data available. However, in order to assess the
306 robustness of the flux estimates, a sensitivity analysis was conducted, based on Equation 3,
307 and presented in Table 2. For this analysis, values of the three parameters K_{sat}, $\mathrm{d}H/\mathrm{d}L$ and L_b
308 were varied between –50% to +50% of the measured/modelled values used to determine the
309 fluxes presented in Section 4.2. The modified values were then used to re-calculate the total
310 annual sub-surface flux (because of the linear form of the equation, varying any of the three
311 parameters by the same proportion has an identical numerical outcome). In addition, fluxes
312 were re-calculated assuming that the length of the hydrologically-active boundary between
313 the moraine complex and the sandur was either constant (at 7000 m, as assumed for the
314 fluxes presented in Section 4.2) or varied linearly, between zero and the seasonal maximum
315 (7000 m) from the start of drainage to 1 July, and from 1 October to end of drainage. From
316 the results given in Table 2, it seems unlikely that the calculated sub-surface flux is in error
317 by an order of magnitude, based on errors in measured/modelled saturated hydraulic
318 conductivity, hydraulic gradient and saturated layer depth. Furthermore, varying the length of
319 the boundary that is hydrologically active has only a minor effect on the calculated fluxes, as
320 its impact is greatest when the rate of sub-surface discharge is smallest: early or late in the
321 melt season, or during the long period of recession flow after the cessation of surface melt.
322
323 ## 5. Discussion:
324 ### 5.1. The annual, proglacial, sub-surface hydrological regime at Finsterwalderbreen
325 The results presented in Section 4 provide quantitative insights into hydrological
326 pathways in proglacial areas underlain by permafrost. The annual cycle in proglacial

atmospheric and surface water fluxes at Finsterwalderbreen was described in detail in Hodgkins et al. (2009). We are able here to develop that description with detail of the variation in sub-surface water fluxes, which are rarely measured in glacierized environments. This description can be used as a context for understanding both the hydrological functioning of high-latitude, glacierized catchments and material fluxes from such catchments (e.g. Wadham et al., 2000; Cooper et al., 2002; Hodgkins et al., 2003).

The annual formation of the active layer commences following the recession of the snowpack, although persistent snow patches may initially delay thawing in some areas. Active layer formation in the Finsterwalderbeen proglacial area is estimated to have commenced around 14 June in 1999. As the melt season proceeds, lake levels in the moraine complex fall in response to the gradual deepening of the active layer and resultant water loss. Consequently, an increasing proportion of runoff is routed from the moraine complex to the sandur via sub-surface flow paths, resulting in the gradual disappearance of many ephemeral surface channels, and a dominant, sub-surface hydraulic gradient from moraine complex to sandur becomes established.

Peak seasonal flow in the proglacial, surface channel network tends to occur in mid-to-late July in this location, in response to high rates of ablation on the lower reaches of the main glacier; it may be accompanied by subglacial outburst floods, submerging the sandur for several days at a time (Wadham et al., 2001). The impact of such events on sub-surface flow is significant, since the dominant hydraulic gradient from the moraine complex to the sandur is temporarily reversed, allowing floodwaters from the proglacial channel network to recharge sub-surface water levels in the active layer at the boundary zone of the moraine complex. During preceding and succeeding periods of lower flow, the hydraulic gradient is maintained from the moraine complex to the sandur, although the gradient beneath the sandur itself is reversed diurnally, in response to diurnal flow variations in the proglacial channel network. The rate of sub-surface discharge from the moraine complex increases as the melt

season proceeds, reflecting the progressive deepening of the active layer and the supply of water from the interior of the moraine complex. A degree of flushing occurs following periods of rainfall, as infiltrating precipitation displaces water stored in the active layer.

The refreezing of the active layer commences in early-to-mid October, as two freezing waves begin to advance: one from the ground surface and one from the permafrost table (Marlin et al., 1993). However, complete refreezing may take 6–8 weeks, since the release of latent heat upon freezing offsets the initial drop in temperature (French, 2007). This temporal pattern appears to be typical for high-latitude, permafrost-influenced catchments. For instance, Humlum (1998) found that seasonal maximum thaw depth in the active layer was reached in late September at Qeqertarsuaq, Greenland (69˚ 15' N, mean annual air temperature –5.1˚ C) and that the closure of the active layer occurred between late December and late January. In the somewhat more northerly Finsterwalderbeen proglacial area, closure is estimated to have occurred around 11 December in 1999 (Fig. 4A).

5.2. The complete (atmospheric, surface and sub-surface) annual proglacial hydrological budget at Finsterwalderbreen

The results presented in this paper, in combination with those presented in Hodgkins et al. (2009), also enable the complete, annual hydrological budget of the proglacial zone to be determined. This allows the relative importance of the various hydrological pathways in the proglacial zone to be identified. The annual, steady-state hydrological budget of the proglacial zone may be represented by the simple water-balance model

$$W_{PZ} = W_P + W_R - W_E - W_{SSS} - W_{SR} \pm \Delta W_S \quad (5)$$

where W_{PZ} is the net proglacial water flux, W_P is the precipitation water flux, W_R is the channel recharge water flux (active-layer discharge from the sandur to the moraine complex),

379 W_E is the evaporation water flux, W_{SSS} is the sub-surface seepage water flux (active-layer
380 discharge from the moraine complex to the sandur), W_{SR} is the surface runoff water flux
381 (mainly snowmelt and lake drainage from the moraine complex) and ΔW_S is the change in
382 water storage. A schematic of this model is presented in Fig. 5, with the addition of both
383 glacial runoff, which effectively constitutes a proglacial throughput, and bulk runoff, which is
384 the sum of glacial runoff and the net proglacial water flux. Specific values of the water
385 balance terms are also given in Table 3. In both cases, the water fluxes given are annual
386 totals, derived from the data presented in this paper and in Hodgkins et al. (2009), with the
387 exception of the value for surface runoff from the moraine complex, which was determined
388 by balance, assuming zero change in water storage.
389 In the year studied, precipitation exceeded evaporation by a little over 80%, though
390 during the summer season, the evaporation rate was almost five times that of precipitation.
391 Runoff was simply determined here as precipitation minus evaporation, as monitoring the
392 extensive network of small, surface streams draining the moraine complex was not a feasible
393 task. The value of runoff (104 mm a^{-1}) is small compared to other Svalbard values given by
394 Killingtveit et al. (2003), though this can be explained by the inclusion of glacial runoff in
395 those other values. However, assuming no significant storage changes, the water budget
396 balances without any obvious difficulties or anomalies, so there is no indication of an
397 apparent precipitation deficit, as identified at some other Arctic catchments: again, this may
398 be partly attributable to the separation of glacial water fluxes from specifically proglacial
399 ones in this study. Killingtveit et al. (2003) considered the main uncertainties in high-latitude
400 water balances to be: (1) the distribution of precipitation, and (2) the rate of evaporation.
401 Regarding (1), the Finsterwalderbreen proglacial area has a limited elevation range (10–50 m
402 a.s.l., the maximum being moraine crests of limited spatial extent), so minimal extrapolation
403 is required, but the hummocky topography of the moraine complex contributes to the
404 relatively large uncertainty in winter precipitation, in particular; this is reflected in the large,

405 proportional error term for the precipitation flux in Fig. 5. Regarding (2), the modelled rate of
406 evaporation from the proglacial area of Finsterwalderbreen (141 mm a^{-1}) compares
407 favourably with other estimates from non-glacierized (and the non-glacierized parts of
408 glacierized) Svalbard catchments, which are in the range 51–200 mm a^{-1} (Jania and Pulina,
409 1994; Killingtveit et al., 1994; Bruland, 2001; Mercier, 2001). Killingtveit et al. (2003)
410 determined average annual evaporation (as a function of air temperature, based on
411 evaporation pan measurements at Ny-Ålesund) for glacier-free areas at three locations in
412 Svalbard to be about 80 mm a^{-1}.

413 The notable exclusion from the water-balance model is the contribution to total, annual
414 glacial runoff by over-winter subglacial drainage. However, a reliable estimate for this value
415 may be derived by calculating the water-equivalent volume of the proglacial icing, which
416 typically accumulates over an area of about 0.3 km^2. Previous coring investigations have
417 revealed that the icing typically has a mean thickness of 1.5 m (Wadham et al., 2000).
418 Assuming an ice density of 900 kg m^{-3}, a water-equivalent volume of about 4.05×10^5 m^3 of
419 winter subglacial drainage is implied. This estimate equates to <1% of average annual glacial
420 runoff and is therefore unlikely to be a significant source of error through its contribution to
421 storage changes. Neither is there any indication of significant changes in active-layer water
422 storage; the magnitude of the sub-surface water flux is an order of magnitude smaller than the
423 atmospheric and surface fluxes, and fully two orders of magnitude smaller than the bulk
424 catchment runoff (Table 3).

425

426 ## 6. Conclusions

427 Understanding the water balance of glacierized catchments is important both for furthering
428 scientific understanding of the hydrological functioning of snow- and ice-fed systems at a
429 time of rapid environmental change, and for the management of snow- and ice-derived water
430 resources of the world's major mountain chains, likewise in the context of change (Barnett et

al., 2005; Bates et al., 2008). Even in high latitudes, remote from centres of population, changes in the storage and release of freshwater may have important implications for the functioning of aquatic ecosystems, ocean currents and ice-sheet stability (Das et al., 2008; Hanna et al., 2008; Mernild et al., 2008; Milner et al., 2009; Schofield et al., 2010).

This contribution has demonstrated that active-layer depth, hydraulic head and specific discharge may be successfully monitored as part of a water balance study in permafrost-influenced catchments. There are a range of practical limitations necessarily associated with monitoring sub-surface processes in remote and relatively intractable areas such as the Finsterwalderbreen catchment in Svalbard, but some aspects of the environment compensate for these: for instance, the air temperature-active-layer depth relationship is very linear, allowing early-season thawing and late-season freezing to be modelled quite straightforwardly. The active layer itself responds quite sensitively to forcing from proglacial surface hydrology, with diurnal reversals of the hydraulic gradient between the moraine complex and the sandur taking place from the mid-melt-season onwards, and clear flux peaks related to rainfall.

The results obtained are consistent with previous water balance studies from Svalbard, though this contribution is distinctive in quantifying active-layer fluxes, although the total annual flux from the moraine complex to the sandur, at 11 mm, is very small compared to the total annual catchment runoff, at 1073 mm. While the total water balance was determined assuming no significant changes in any plausible stores, the consistency of the various measured or estimated values for the balance components suggests there are unlikely to be significant gains from or losses to storage in the active layer. Uncertainties in the sub-surface variables are difficult to quantify, although given the small magnitude of the annual totals, are unlikely to have an important effect on the water balance calculation. Probably the principal source of uncertainty is the representativeness of the location used for well monitoring: this is essentially a matter of judgement. In any case, it is clear that throughputs from the adjacent

457 glacier – 1697 mm of runoff in the season studied (Hodgkins et al., 2009) – dominate the
458 proglacial area hydrologically, underlining the important role of glacially-derived water
459 fluxes in this high-latitude region.
460

Acknowledgments

We are extremely grateful to Professor Kurt Roth (Institute of Environmental Physics, University of Heidelberg, Germany), and Dr Julia Boike (Alfred Wegener Institute for Polar and Marine Research, Germany) for providing data that enabled the freeze-back of the active layer to be modelled. This work was funded by the NERC ARCICE Thematic Programme grant GST/02/2204 and tied studentship GT24/98/ARCI/8. We would like to thank the Norsk Polarinstitutt for logistical support and Deborah Jenkins, Elizabeth Farmer, Andrew Terry and Catherine Styles for assistance in the field.

References

ACIA. 2004. Impacts of a Warming Arctic: Arctic Climate Impact Assessment. Cambridge, Cambridge University Press.

Barnett, T.P., Adam, J.C., Lettenmaier, D.P. 2005. Potential impacts of a warming climate on water availability in snow-dominated regions. Nature 438, 303–309.

Bates, B.C., Kundzewicz, Z.W., Wu, S., Palutikof, J.P. (Eds). 2008. Climate Change and Water. Technical Paper of the Intergovernmental Panel on Climate Change, IPCC Secretariat, Geneva, 210 pp.

Boike, J., Roth, K., Overdain, P.P. 1998. Thermal and hydrologic dynamics of the active layer at a continuous permafrost site (Taymyr Peninsula, Siberia). Water Resources Research 34, 355–363.

Booji, M., Leijnse, A., Haldorsen, S., Heim, M., Rueslåtten, H. 1998. Subpermafrost groundwater modelling in Ny-Ålesund. Nordic Hydrology 29, 385–396.

Bouwer, H., Rice, R.C. 1976. A slug test for determining hydraulic conductivity of unconfined aquifers with completely or partially penetrating wells. Water Resources Research 12, 423–428.

Bouwer, H. 1989. The Bouwer and Rice slug test – an update. Groundwater 27, 304–309.

Bruland, O., Marechal, D., Sand, K., Killingtveit, Å. 2001. Energy and water balance studies of a snow cover during snowmelt period at a high arctic site. Theoretical and Applied Climatology 70 (1–4), 53–63.

Cooper, R.J., Wadham, J.L., Tranter, M., Hodgkins, R., Peters, N. 2002. Groundwater hydrochemistry in the active layer of the proglacial zone, Finsterwalderbreen, Svalbard. Journal of Hydrology 269, 208–223.

Das, S.B., Joughin, I., Behn, M.D., Howat, I.M., King, M.A., Lizarralde, D, Bhatia, M.P. 2008. Fracture propagation to the base of the Greenland Ice Sheet during supraglacial lake drainage. Science 320, 778–781.

Førland, E.J., Hanssen-Bauer, I., Nordli, P.Ø. 1997. Climate statistics and longterm series of temperature and precipitation at Svalbard and Jan Mayen. Klima 21/97. Oslo, Norwegian Meteorological Institute.

French, H.M. 2007. The Periglacial Environment (3rd Edition). Wiley, Chichester.

Hagen, J.O., Kohler, J., Melvold, K., Winther, J.-G. 2003. Glaciers in Svalbard: mass balance, runoff and freshwater flux. Polar Research 22, 145–159.

Haldorsen, S., Heim, M. 1999. An arctic groundwater system and its dependence upon climatic change: an example from Svalbard. Permafrost and Periglacial Processes 10, 137–149.

Haldorsen, S., Heim, M., Lauritzen, S.-E. 1996. Subpermafrost groundwater, western Svalbard. Nordic Hydrology 27, 57–68.

Hanna, E., Huybrechts, P., Steffen, K., Cappelen, K., Huff, R., Shuman, C., Irvine-Fynn, T., Wise, S., Griffiths, M. 2008. Increased Runoff from Melt from the Greenland Ice Sheet: A Response to Global Warming. Journal of Climate 21, 331–341.

Hanssen-Bauer, I., Kristensen Solås, M., Steffensen, E.L. 1990. The Climate of Spitsbergen. Norsk Meteorologiske Institutt Rapport 39/90.

Harding, R.J., Lloyd, C.R. 1997. Fluxes of water and energy from three high latitude tundra sites in Svalbard. Nordic Hydrology 29, 267–284.

Herz, K., Andreas, G. 1966. Untersuchungen zur ökologie der periglazialen Auftauschicht im Kongsfjordgebiet (Westspitzbergen). Petermanns Geographische Mitteilungen 110, 260–274.

Hodgkins, R., Cooper, R., Wadham, J., Tranter, M. 2009. The hydrology of the proglacial zone of a high-Arctic glacier (Finsterwalderbreen, Svalbard): Atmospheric and surface water fluxes. Journal of Hydrology 378, 150–160.

Hodson, A., Gurnell, A., Washington, R., Tranter, M., Clark, M., Hagen, J.O. 1998. Meteorological and runoff time-series characteristics in a small, high-Arctic glaciated basin, Svalbard. Hydrological Processes, 12, 509–526.

522 Humlulm, O. 1998. Active layer thermal regime 1991–1996 at Qeqertarsuaq, Disko Island,
523 central West Greenland. Arctic and Alpine Research 30(3), 295–305.
524 Jania, J., Pulina, M. 1994. Polish hydrological studies in Spitsbergen, Svalbard: a review of
525 some results. In Sand, K., Killingtveit, Å., eds. Proceedings of the 10th International
526 Northern Research Basins Symposium and Workshop, Spitsbergen, Norway, 47–76.
527 SINTEF Report 22 A96415. Trondheim, Norwegian Institute of Technology.
528 Killingtveit, Å, Petterson, L.-E., Sand, K. 1994. Water balance studies at Spitsbergen,
529 Svalbard. In Sand, K., Killingtveit, Å., eds. Proceedings of the 10th International
530 Northern Research Basins Symposium and Workshop, Spitsbergen, Norway, 77–94.
531 SINTEF Report 22 A96415. Trondheim, Norwegian Institute of Technology.
532 Killingtveit, A., Pettersson, L.-E., Sand, K. 2003. Water balance investigations in Svalbard.
533 Polar Research, 22(2), 161–174.
534 Marlin, C., Dever, L., Vacier, P., Courty, M.-A. 1993. Variations chimiques et isotopiques de
535 l'eau du sol lors de la reprise en gel d'une couche active sur perigélisol continu
536 (Presqu'île de Brögger, Svalbard). Canadian Journal of Earth Sciences 30, 806–813.
537 Meehl, G.A., Stocker, T.F., Collins, W.D., Friedlingstein, P., Gaye, A.T., Gregory, J.M.,
538 Kitoh, A., Knutti, R., Murphy, J.M., Noda, A., Raper, S.C.B., Watterson, I.G., Weaver,
539 A.J., Zhao, Z.-C. 2007. Global Climate Projections. In Solomon, S., D. Qin, M.
540 Manning, Z. Chen, M. Marquis, K.B. Averyt, M. Tignor and H.L. Miller, eds. Climate
541 Change 2007: The Physical Science Basis. Contribution of Working Group I to the
542 Fourth Assessment Report of the Intergovernmental Panel on Climate Change.
543 Cambridge University Press, Cambridge, United Kingdom and New York, NY, USA.
544 Mercier, D. 2001. Le Ruisellement au Spitsberg. Clermont-Ferrand, France, Blaise Pascal
545 University Press.
546 Mernild, S.H., Liston, G.E., Hasholt, B. 2008. East Greenland freshwater runoff to the
547 Greenland-Iceland-Norwegian Seas 1999–2004 and 2071–2100. Hydrological

548 Processes 22, 4571–4586.
549 Milner, A.M., Brown, L.E., Hannah, D.M. 2009. Hydroecological response of river systems
550 to shrinking glaciers. Hydrological Processes 77, 62–77.
551 Pecher, K. 1994. Hydrochemical analysis of spatial and temporal variations of solute
552 composition in surface and subsurface waters of a high arctic catchment. Catena, 21,
553 305–327.
554 Roth, K., Boike, J. 2001. Quantifying the thermal dynamics of a permafrost site near Ny-
555 Ålesund, Svalbard. Water Resources Research, 37, 2901–2914.
556 Schofield, O., Ducklow, H.W., Martinson, D.G., Meredith, M.P., Moline, M.A., Fraser, W.R.
557 2010. How Do Polar Marine Ecosystems Respond to Rapid Climate Change? Science
558 328, 1520–1523.
559 Stäblein, G. 1971. Der polare Permafrost und die Auftauschicht in Svalbard. Polarforschung
560 41, 112–120.
561 Wadham, J.L., Tranter, M., Dowdeswell, J.A. 2000. Hydrochemistry of meltwaters draining a
562 polythermal-based, high-Arctic glacier, south Svalbard: II. Winter and early Spring.
563 Hydrological Processes, 14, 1767–1786.
564 Wadham, J.L., Cooper, R.J., Tranter, M., Hodgkins, R. 2001. Enhancement of glacial solute
565 fluxes in the proglacial zone of a polythermal glacier. Journal of Glaciology 47 (158),
566 378–386.
567 Warburton, J. 1999. Environmental change and sediment yield from glacierised basins: the
568 role of fluvial processes and sediment storage. In Brown, A.G., Quine, T.A., eds.
569 Fluvial Processes and Environmental Change. Wiley, Chichester, 363–384.
570 Zemp, M., Roer, I., Kaeaeb, A., Hoelzle, M., Paul, F., Haeberli, W. 2008. Global glacier
571 changes: facts and figures. UNEP and WGMS, Nairobi and Zurich.
572

573 ## Figure captions

574

575 Fig. 1. Location of the study site within the Svalbard archipelago (inset) and configuration of
576 the Finsterwalderbreen proglacial area (main). The limits of the moraine complex are shown
577 with a solid white line; the part of the moraine complex that drains to the sandur is delimited
578 by the long-dashed line; the boundary between the moraine complex and sandur is shown by
579 the short-dashed line. WT marks the position of the wells transect, along which five wells are
580 located (Fig. 2A). Aerial photograph acquired by UK Natural Environment Research Council
581 Airborne Research and Survey Facility in 2003.

582

583 Fig. 2. (A) Detail map of the wells transect, located in Fig. 1. Wells 1 and 2 behave so
584 similarly to Well 3 that their data are excluded from subsequent figures, for clarity. (B)
585 Example of a monitoring well, comprising a pair of rigid, plastic tubes, the bottoms of which
586 are sealed; the buried length of each tube features a screened intake into which sub-surface
587 waters can flow. One tube was used for water sampling for hydrochemical studies (Cooper et
588 al., 2002), while the monitoring instruments described in the text are secured at the bottom of
589 the other tube: further details are given in Cooper et al. (2002).

590

591 Fig. 3. Temporal variation in (A) hydraulic head and (B) specific discharge during the period
592 of monitoring. Well 4 is in the transitional zone between the moraine complex and the
593 sandur; Well 5 is representative of the former, Well 3 of the latter. Note that positive values
594 indicate discharge from the moraine complex to the sandur and negative values indicate
595 recharge from the sandur to the moraine complex.

596

597 Fig. 4. Proglacial active layer depth/thickness (A) and daily sub-surface water flux between
598 the moraine complex and sandur (B). Note that positive values indicate discharge from the

599 moraine complex to the sandur and negative values indicate recharge in the opposite
600 direction.
601
602 Fig. 5. Schematic representation of the complete, annual water budget for the
603 Finsterwalderbreen proglacial area. Blue arrows represent inputs, red arrows represent
604 outputs, and other arrows represent internal transfers; broken lines represent minor multi-
605 directional, stores/exchanges that cannot be quantified from the data available. All of the
606 water fluxes presented in the figure are given in m^3, with estimates of probable error, except
607 for channel recharge, active-layer discharge and surface runoff, for which it is not possible to
608 determine realistic error estimates with the data available: these fluxes must therefore be
609 viewed as first-order estimates. The determination of errors in all other water fluxes are
610 described in detail in Hodgkins et al. (2009), with additional estimates as follows: (1) the
611 error for the precipitation water flux is an average of probable errors previously determined
612 for the rainfall and snowpack water-equivalent fluxes, weighted by proportion of total
613 precipitation; (2) the probable error for the glacial runoff water flux is an average, weighted
614 in proportion to overall contribution, of probable errors from the Terminus East and West
615 gauging stations (average-weighted by time, as these errors varied temporally: Hodgkins et
616 al., 2009) and the supraglacial water flux determined from ablation measurements.

Figure 1 (black/white)
Click here to download high resolution image

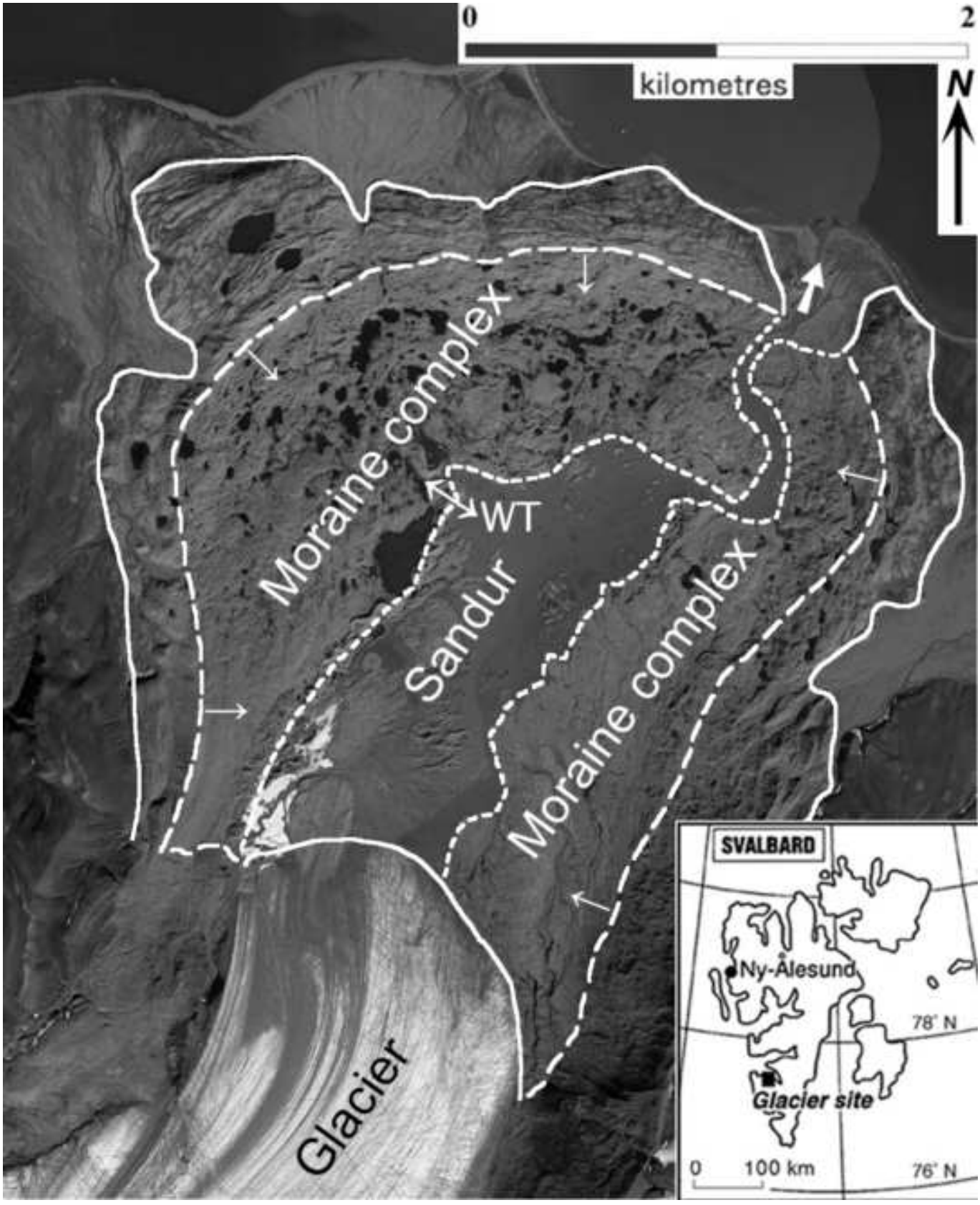

Figure 1 (colour)
Click here to download high resolution image

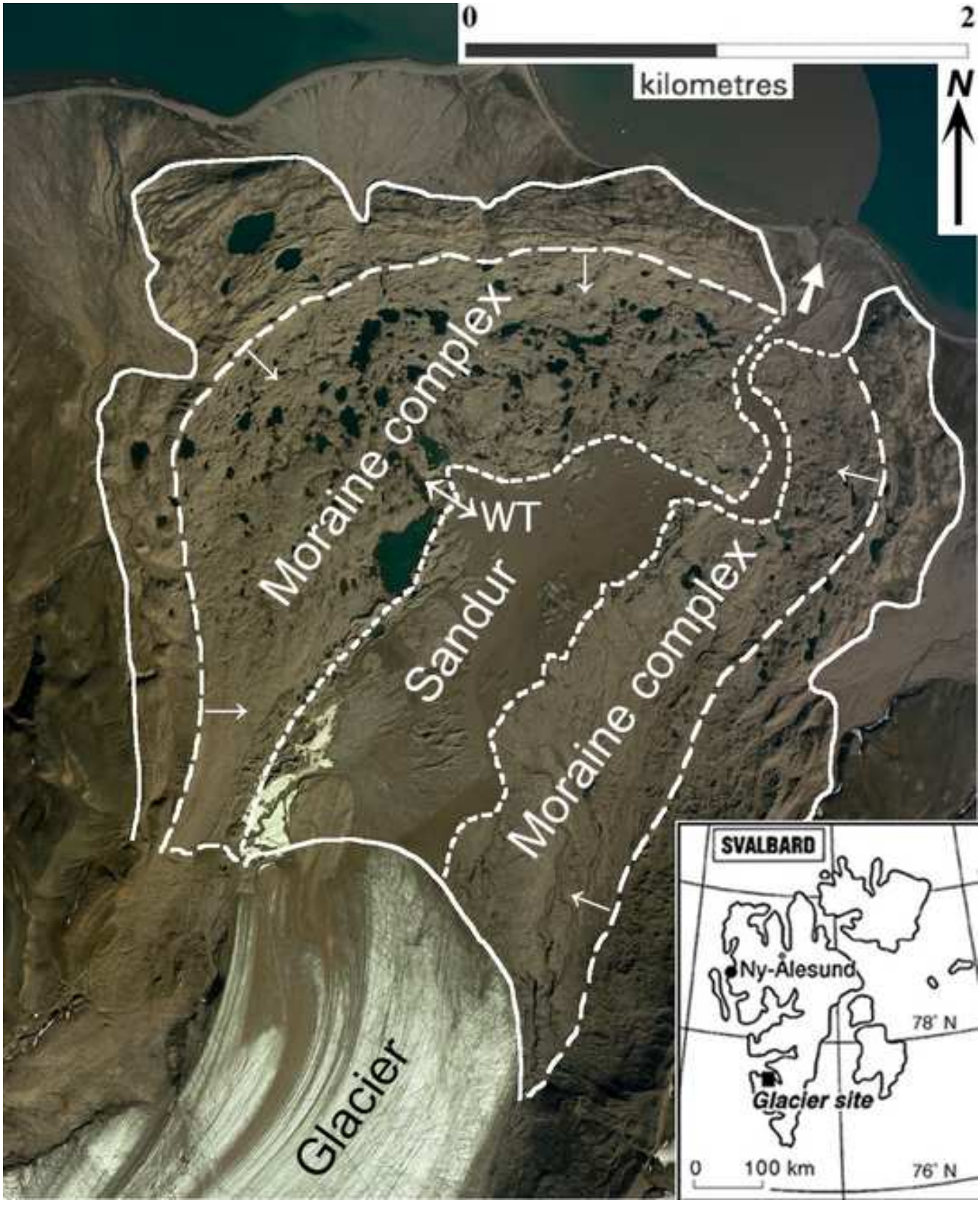

Figure 2 revised (black/white)
Click here to download high resolution image

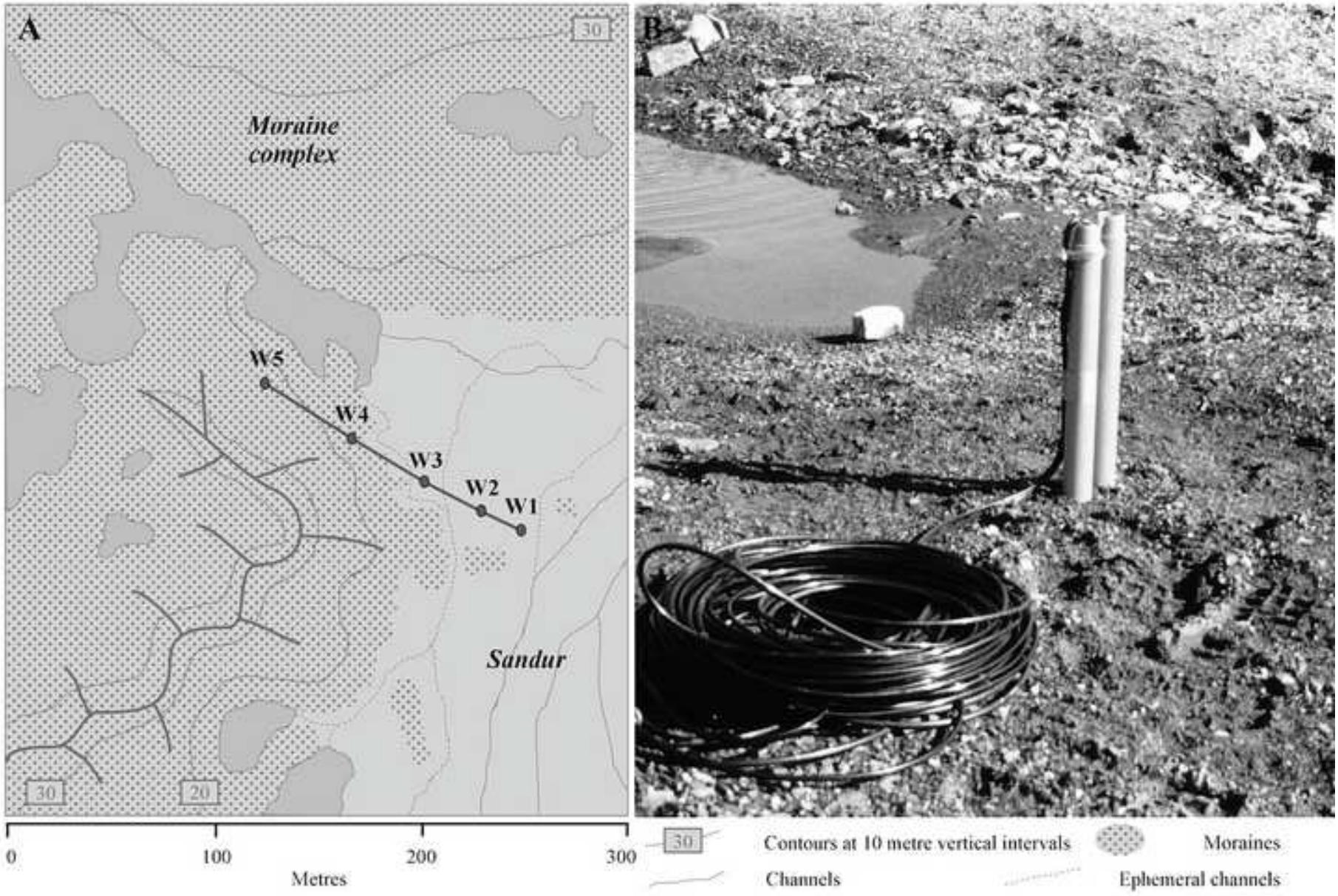

Figure 2 revised (colour)
Click here to download high resolution image

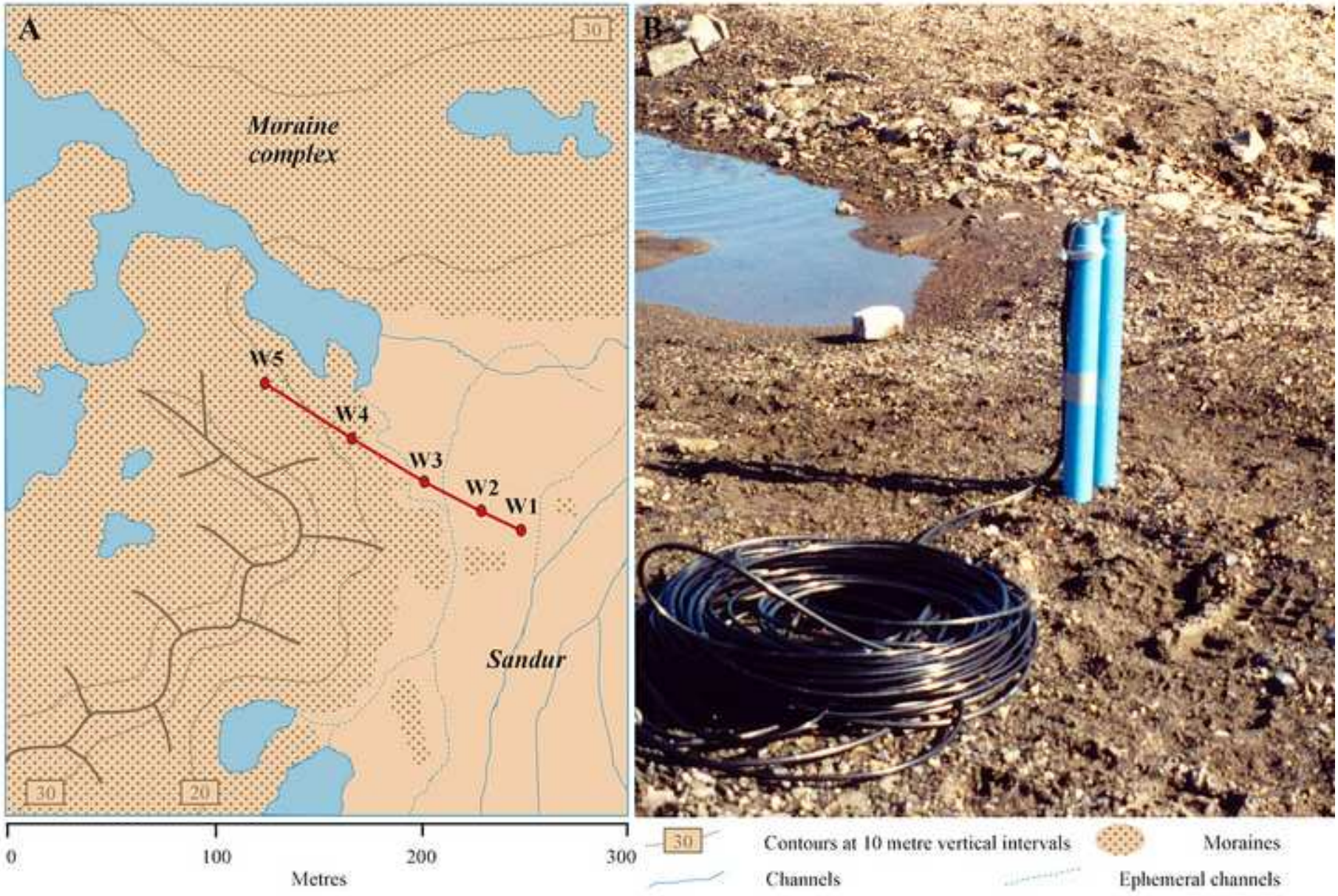

Figure 3 revised
Click here to download high resolution image

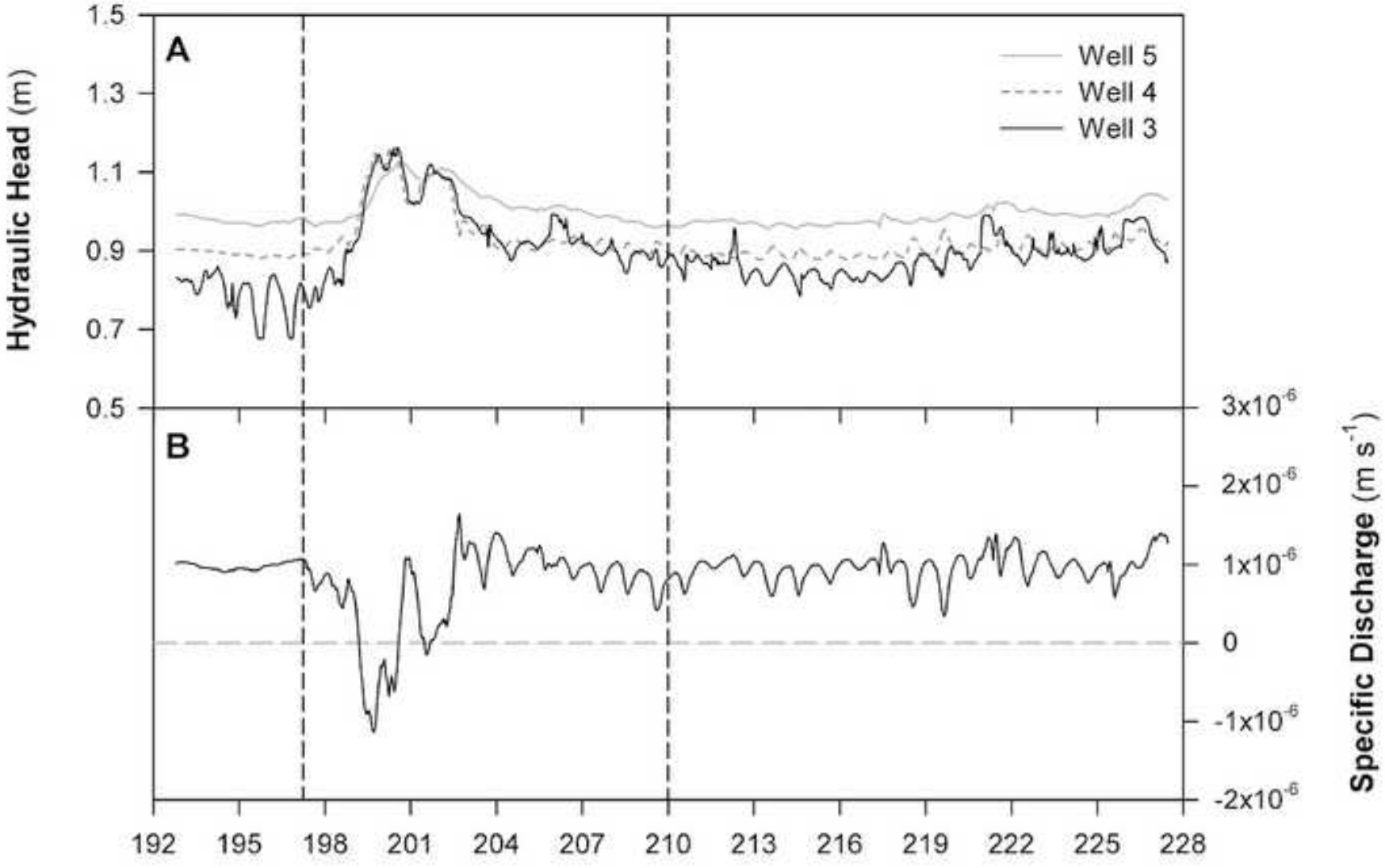

Figure 4
Click here to download high resolution image

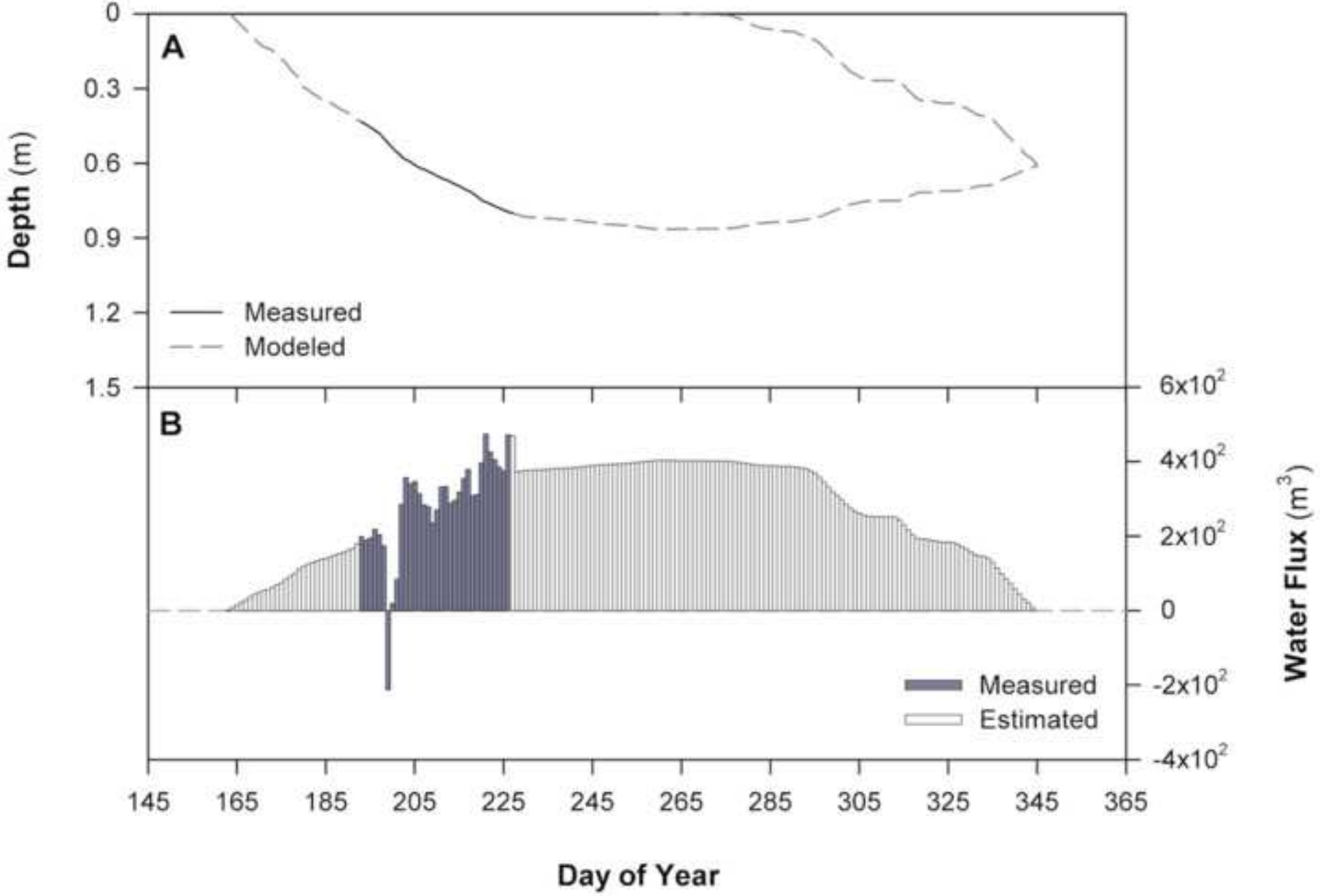

Figure 5 (black/white)
Click here to download high resolution image

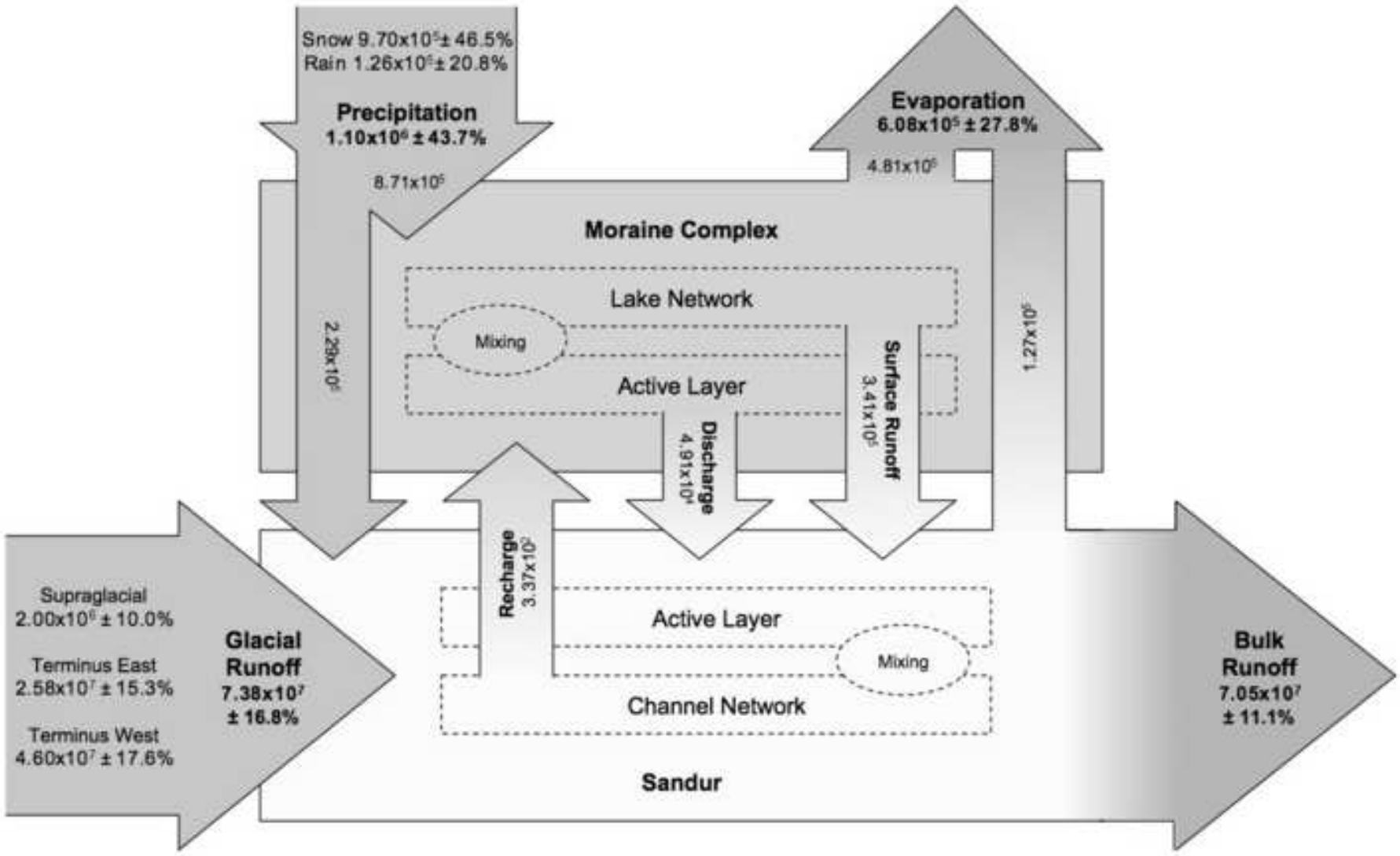

Figure 5 (colour)
Click here to download high resolution image

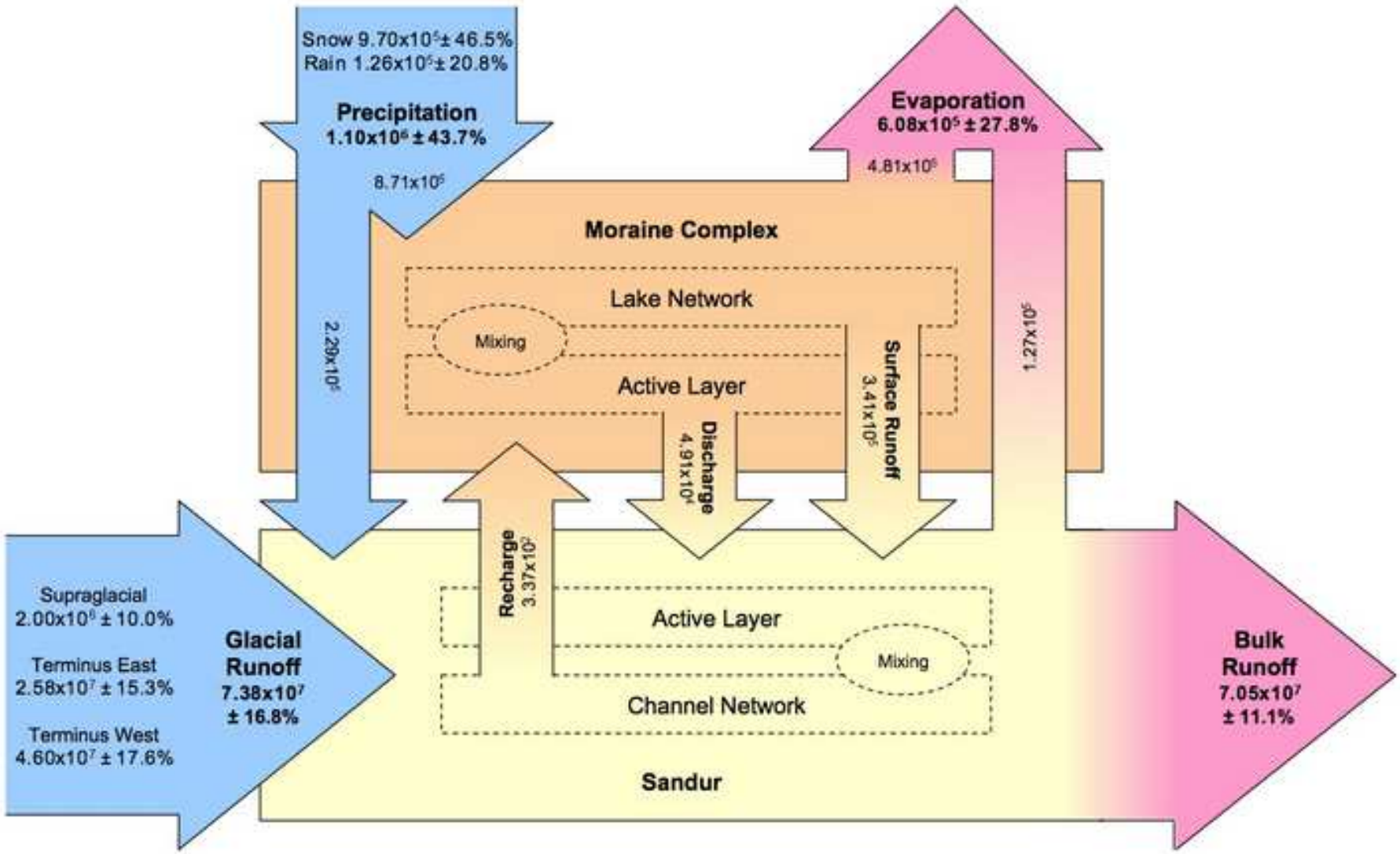

Tables

Table 1: Linear regression models used to predict active- and saturated-layer depths (L_a and L_b respectively) during unmonitored intervals at the start and end of the 1999 melt season. All coefficients are significant at $p<0.05$. T_a is hourly air temperature, positive or negative.

Independent variable	Dependent variable	Slope	Intercept	R^2	When applied
L_a	L_b	1.047	–0.134	0.981 ($n=690$)	For duration of active layer formation
$\sum T_a^+$	L_a	0.012	–0.380	1.000 ($n=2$)	During active-layer thawing
$\sum T_a^-$	L_a	-2.624×10^{-4}	0.000	0.837 ($n=5$)	During active-layer freezing (surface-down)
$\sum T_a^-$	L_a	1.111×10^{-4}	1.179	0.635 ($n=3$)	During active-layer freezing (bottom-up)

Table 2: Sensitivity analysis of sub-surface water flux using equation 3, for the entire period of sub-surface flow (monitored and modelled fluxes, from June to December).

	Constant boundary	Variable boundary
Results using parameter values given in text		
Total annual flux	4.91×10^{4} m^3	4.19×10^{4} m^3
Mean annual discharge	$3.12\pm1.56\times10^{-3}$ m^3 s^{-1}	$2.66\pm1.77\times10^{-3}$ m^3 s^{-1}
Corresponding results with any of K_{sat}, dH/dL or L_b modified by stated percentage		
+50%	7.36×10^{4} m^3 $4.68\pm2.34\times10^{-3}$ m^3 s^{-1}	6.29×10^{4} m^3 $4.00\pm2.66\times10^{-3}$ m^3 s^{-1}
+30%	6.38×10^{4} m^3 $4.06\pm2.02\times10^{-3}$ m^3 s^{-1}	5.45×10^{4} m^3 $3.46\pm2.31\times10^{-3}$ m^3 s^{-1}
+20%	5.89×10^{4} m^3 $3.75\pm1.87\times10^{-3}$ m^3 s^{-1}	5.03×10^{4} m^3 $3.20\pm2.13\times10^{-3}$ m^3 s^{-1}
–20%	3.93×10^{4} m^3 $2.50\pm1.25\times10^{-3}$ m^3 s^{-1}	3.35×10^{4} m^3 $2.13\pm1.42\times10^{-3}$ m^3 s^{-1}
–30%	3.44×10^{4} m^3 $2.19\pm1.09\times10^{-3}$ m^3 s^{-1}	2.93×10^{4} m^3 $1.87\pm1.24\times10^{-3}$ m^3 s^{-1}
–50%	2.45×10^{4} m^3 $1.56\pm0.78\times10^{-3}$ m^3 s^{-1}	2.10×10^{4} m^3 $1.33\pm0.89\times10^{-3}$ m^3 s^{-1}

Table 3: Finsterwalderbreen proglacial area annual water balance, 1999: summary.

Component	Value
Precipitation (winter)	226 mm
Precipitation (summer)	29 mm
Precipitation (total)	256 mm
Evaporation	141 mm
Precipitation - evaporation	115 mm
Surface runoff	104 mm (inferred)
Sub-surface discharge from moraine complex to sandur	11 mm
Sub-surface recharge from sandur to moraine complex	0.1 mm
Glacial runoff	1697 mm (43.5 km^2 glacierized area)
Bulk catchment runoff	1073 mm (65.7 km^2 total catchment area)